The Nucleus **47**, No. 3 (2010)

The Nucleus
A Quarterly Scientific Journal of Pakistan Atomic Energy Commission
NCLEAM, ISSN 0029-5698

PREDICTING THE VARIABILITY IN THE WAVELENGTH STRUCTURES OF THE INCOMING RADIATION DUE TO OZONE LAYER DEPLETION AT ARABIAN SEA

M.A.K. YOUSUF ZAI, J. QUAMAR, J. IQBAL, M.R.K. ANSARI and M.A. HUSSAIN

Department of Applied Physics and Institute of Space and Planetary Astrophysics, University of Karachi, Karachi - 75270, Pakistan

(Received January 22, 2008 and accepted in revised form July 02, 2010)

In this communication we have investigated the variability in the wavelength structures of the radiation due to ozone layer depletion (OLD) using empirical modeling approach. A model has been developed for evaluating sea surface temperature using stratospheric ozone filter. This filter has been formulated taking into account of the ozone layer depletion (OLD) strategy for Pakistan atmospheric regions. For making predictions of various wavelength, stochastic analysis is implemented here for observing future prospects of the coming radiation. These predictions are useful for public, private and government organizations.

Keywords: Variability, Ozone layer depletion, Max.wavelength of emission, Stratospheric region

1. Introduction

Ozone in the stratosphere acts to protect our biosphere from harmful ultraviolet (UV) radiation from the sun. UV radiation in human and other animals can cause sunburn, cell damage, skin cancers and promotion of AIDS viruses. Plants and other simpler organisms such as phytoplankton are also susceptible to UV damage reducing their productivity rates [1-3, 6,7] The UV region of the electromagnetic spectrum consists of UV-A with wavelengths over 320 nm; UV-B with wavelengths from 290 nm to 320 nm, and UV-C at less than 290 nm. The UV-A is least damaging having the lowest energy; while UV-C is normally not present at the ground level as it is absorbed in the atmosphere. Some portion of the UV-B is absorbed by the ozone layer and the remaining portion is the most damaging biologically and the region that is increasing as the protective ozone layer is depleted. These wavelengths have sufficient energy to disrupt bond in DNA and certain other proteins. A Small reduction in ozone concentration can lead to large increases in the amount of UV reaching the earth [4,8-10].

It is well known fact that the efficiency of the ozone shield is subject to a continuous change because of various natural and non-natural causes. This situation allows a penetration of ultra violet radiation through the earth's atmosphere where most of the processes involved such as variations in temperature and the wavelength of incoming radiation are physical in their nature. These physical processes produce changes in stratospheric chemical composition also, creating a situation that is hazardous to human population directly and indirectly. In this communication we will study the variability in the wavelength of radiation and the prediction equation using the process of the filtration of solar UV radiation through constructed ozone filter and constructing a mathematical model for sea surface temperature to determine the variation in the temperature. Using temperature variations, the variations in the wavelength structures will be discussed. Probabilistic and stochastic models can also be implemented for a more accurate study. This study is important from the point of view of monitoring OLD effects on marine organisms on which our future economy will be based [5, 11-14].

2. Filtration of Solar UV Radiation Through Ozonosphere

As we know that the change in ozone concentration, in turn alters the change in temperature. The direct radiative effect of gases comes about via absorption of solar radiation and absorption and emission of long wave radiation also referred to as thermal, terrestrial, or infrared.

The temperature does refer to heat intensity. For a discrete body, the temperature is proportional to the average kinetic energy of the component molecules. Solar radiation reaching the sea level consists of broad range of wavelengths or frequencies. Among this radiation, the optical wavelengths are entirely responsible for heating of the earth's atmosphere, land surface and oceans.

The chemical reactions for the formation and annihilation of ozone in the stratosphere are given below:

$$O_2 + h\nu\ (\lambda < 240\text{ nm}) \rightarrow O + O \qquad \text{Slow} \qquad (1)$$

$$O + O_2 + M \rightarrow O_3 + M \qquad \text{Fast} \qquad (2)$$

In which M is the third body required to carry off excess energy of the association process.

$$O_3 + h\nu(\lambda < 310\text{ nm}) \rightarrow O + O_2 \qquad \text{Fast} \qquad (3)$$

$$O + O_3 \rightarrow O_2 + O_2 \qquad \text{Slow} \qquad (4)$$

Overall reaction is as follows:

$$O + O_3 \rightarrow 2\,O_2 \qquad (5)$$

Calculations of the variation of temperature can provide information about the chemical reactions taking place in the stratospheric region [13].

3. Quantification of Ultraviolet Flux

We know that stratosphere will act as the secondary source of UV radiation through the ozone filter. The UV flux reaching the Arabian Sea is given by the following expression [14-15].

$$P_n = \left(1 - \frac{V_n}{V_t}\right) \qquad (6)$$

V_n = nth Volume of the ozone column at Stratospheric region of Pakistan

V_t = Total Volume of ozone at Stratospheric region of Pakistan

n is the total # of observations.

$$P_n \times \text{Luminosity} = f_{effective} \qquad (7)$$

$$F = \frac{f_{effective}}{4\pi R^2_{\text{Arabian sea}}}. \qquad (8)$$

The Eq (6) characterizes the ozone filter for different luminosities that have been calculated using the UV- Lyman flux of solar radiation and effective luminosity reaching the Arabian sea through the ozone filter respectively. The Eq (8) gives the values of UV-B flux reaching Arabian Sea. Figure.1 depicts the variation of UV-B. Along the y-axis, the abbreviations F.R.A.S., stands for Flux Reaching Arabian Sea in watts / meter square.

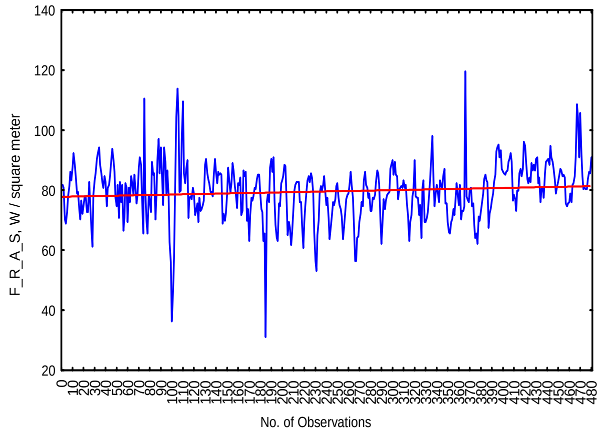

Figure 1. Variation of UV flux versus time, depicting the enhancement and decrease of flux due to depletion of O_3 at Pakistan's stratosphere

X- axis indicates the monthly variation of flux in W/m^2 in figure 1 and monthly variation in the computed temperature (^oC) in figure 2 also .

We have constructed a very simple and applied meteorological model that concerns the estimation of the planetary temperature.

The total radiant energy flux from the sun, just outside the earth's atmosphere is 1.353 kW m^{-2}.

The total heat inflow to earth from the sun =

$$\frac{\pi}{4} D^2.\text{Flux} \qquad (9)$$

$$\text{The total heat outflow} = \pi D^2 \sigma T^4 \qquad (10)$$

Where $\sigma = 5.672 \times 10^{-11}$ kW / m^2 K^4, and D is the diameter of the earth considered to be 12.75×10^6m.

The total heat radiated to outer space would be the amount of heat given by Eq (10) plus the amount of heat produced on earth by nuclear decay and tidal friction with the moon, which together are less than 0.1 percent of the solar energy inflow and can be safely ignored. The outward radiation is calculated using the surface area rather than the projected area. T can then be determined by equating the expressions of heat inflow and heat outflow as follows:

$$\text{Heat flow in} = \frac{\pi}{4}D^2.\text{Flux} = \text{heat flow out} = \pi D^2\,\sigma\,T^4$$

$$T=\left(\frac{\text{Flux}}{4\sigma}\right)^{0.25} \tag{11}$$

Where the flux in Eq. (11) is the flux reaching the Arabian sea through ozone filter. Using Eq (11) the approximate value of the temperature of the earth's surface can be computed.

4. Stochastic Model for Sea Surface Temperature

We have constructed a stochastic model for OLD data. We have also shown that AR(1) model as depicted in Eq (12)

$$X_t = \beta_1 X_{t-1} + \alpha_t \tag{12}$$

is most adequate for OLD study. Now we will use this model to study sea surface temperature. Here $\hat{\beta}_1$ comes out to be $X_t = \beta_1 X_{t-1} + \alpha_t$ 0.69 ± 0.035 and the Mean Sum of Squared Errors (MSSE) $\hat{\sigma}_a^2$ appears as 11.64 ± 1.9, $\hat{\rho}$ (α_t and α_{t-1}) and $\hat{\rho}$ (α_t and X_{t-2}) comes out to be – 0.015 and 0.0012 respectively.

There may exist temporal and spatial limitations of our model (12) as a representation of the real stratospheric atmosphere [7-9]. O_3 depth fluctuations seem to be transported alongwith seasonal variations (cf. Figure 2) to Pakistan's atmospheric regions. Moreover, the O_3 layer variability forms an O_3 filter in the passage of UV-B that also gives a variation in temperature.

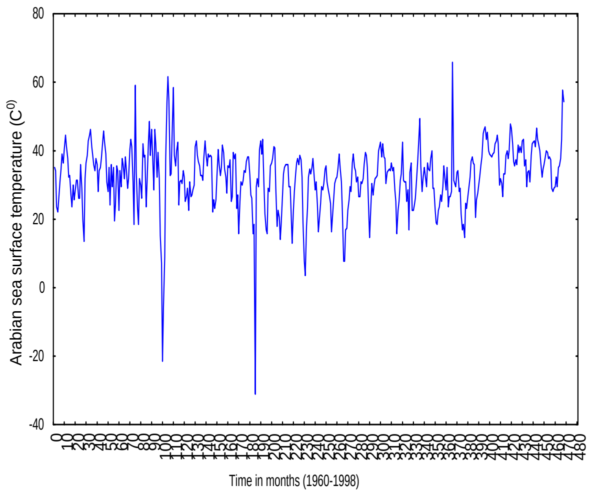

Figure 2. The plot of Arabian Sea surface temperature vs. time Jan. 1960-Dec.1998 that exhibits the variation in temperature due to Ozone Layer Depletion (OLD).

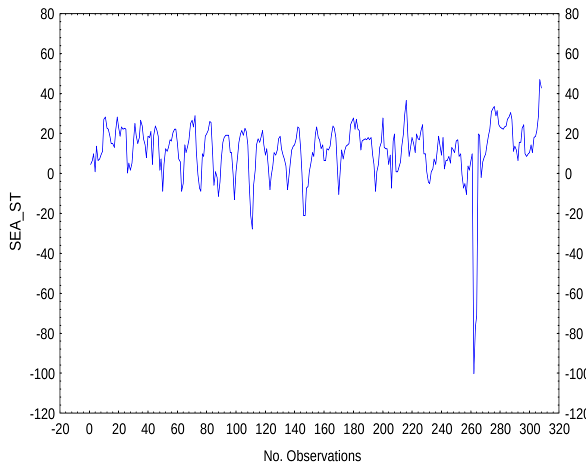

Figure 3. Residual plot elucidating the appropriateness of the constructed model for sea surface temperature.

The residual analysis is depicted in Figure 3 that amply demonstrates that the constructed model is reasonably adequate. The line spectrum or periodogram (cf Figure 4) constructed to identify the randomness in the Sea Surface Temperature due to Ozone Layer Depletion (OLD).

Error structure can be revealed by the autocorrelation for residuals of the O_3 depth events exhibiting a rather neat serial correlation (vide Figure.5). The predicted value comfortably establishes the validity of the constructed model (cf. Figure 6).

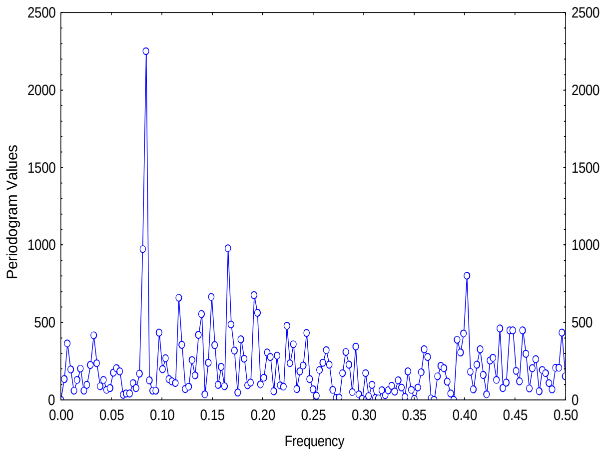

Figure.4. Periodogram for Sea Surface Temperature for AR(1) model identifying the randomness due to Ozone Layer Depletion

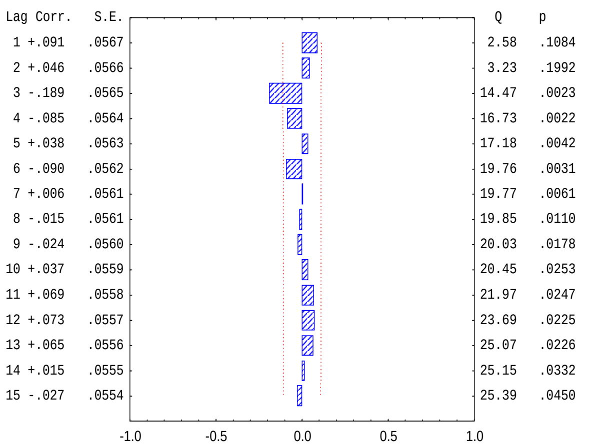

Figure 5. Autocorrelation or serial correlation for Sea Surface Temperature between i^{th} Observations and the $(i+m)^{th}$, exhibiting high degree of correlation.

Substituting α_t = 11.64 ± 1.91 in Eq(12) the forecast of the sea surface temperature for the month of January 1999 is 40.62 ^{o} C . The forecast accuracy is 13.5.% as absolute percentage forecast error (APFE), which is reasonable for Pakistan's atmospheric region.

5. Ozone Layer Depletion(OLD) and Variation in the Wavelength Structure of the Incoming Radiations

We now use the above model in Eq (12) to investigate the variation in the wavelength structure of the incoming radiations due to Ozone Layer Depletion(OLD) with respect to temperature variation at the surface of the earth.

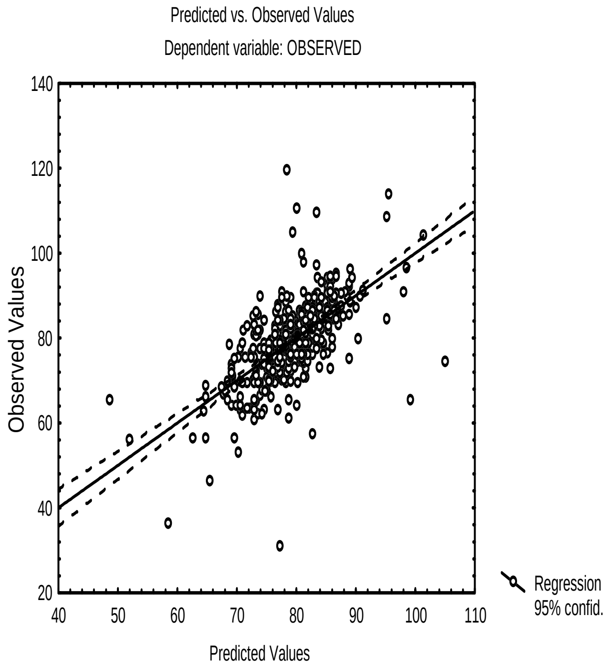

Figure 6. Comparison of observed and predicted values of the Sea Surface temperature showing the behaviour of the constructed model X-axis predicted values of temperature in ^{o}C Y-axis observed values of temperature in ^{o}C.

As we know the change in ozone concentration, changes the temperature. The direct radiative effect of gases comes about via absorption of solar radiation and absorption and emission of long wavelength radiation also referred to as thermal, terrestrial, or infrared radiation. For wavelengths shorter than 0.28μ, the internal transitions involve shifts of electrons in their orbits around the nuclei of one or more of the atoms that make up the molecule, but do not produce any change in the relation of one atom to another within the molecule. Whereas, for wavelengths longer than 1 μ, the changes are not within the individual atoms but are those associated with the vibration of various atoms in the molecule, relative to each other.

In the 0.28μ to 1μ window, photons have too little energy to cause shifts of electron orbits, and too much energy to be in resonance with intra molecular vibrations (for the molecules in air). The absorption peaks of H_2O are caused by various intra molecular vibration modes of the water molecule (3-fundamental vibrations, and overtones).

The distinct features of a black body show that radiant energy is distributed over a range of wavelengths that is narrower for hotter bodies. Wien's law for black body radiation stated that

$$\lambda_{max} = \frac{2.987 \times 10^3 \mu m.K}{T} \tag{13}$$

Where λ_{max} is the wavelength of maximum emission. It exhibits that for the sun surface temperature of about 6000^o K, the peak intensity is at 0.50 μ, corresponding to the visible light. For the earth's surface temperature of about 288^o K the peak intensity is at 10.3μ, which is the infrared region. In fact these are the invisible rays and it can be remarked that though we can not see the earth glowing in the dark, however, with an infra red sensing eye it could be observed. It means that though the sun's energy reaches the earth mostly as visible light, the earth reflects an appreciable amount of energy as infra red radiation. Figures 2 and 8 expose the aspects of variation of sea surface temperature and maximum wavelength emission of our bolometric analysis of the sun and the earth. Figure 7 depicts the distribution of maximum wavelength of emission to appraise the behaviour of the data points that emerge to come from normal distribution.

Similarly, Figure 9 illustrates distribution of maximum wavelengths of emission due to ozone layer depletion that manifests near Gaussian behaviour. Trend equation is given below :

28.66 + 2.93^x

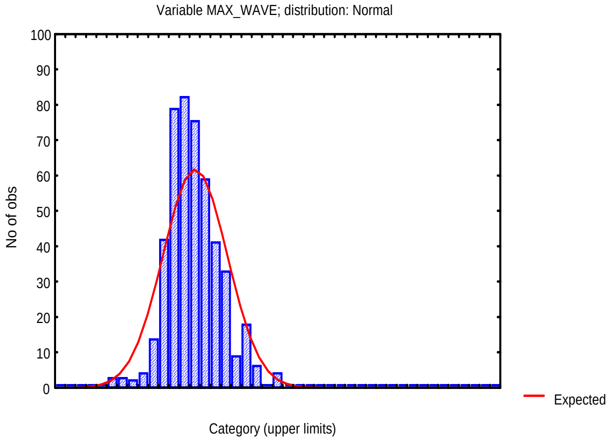

Figure 7. Kolmogorov-Smirnov test to assess how well the data set appears to come from normal distribution.

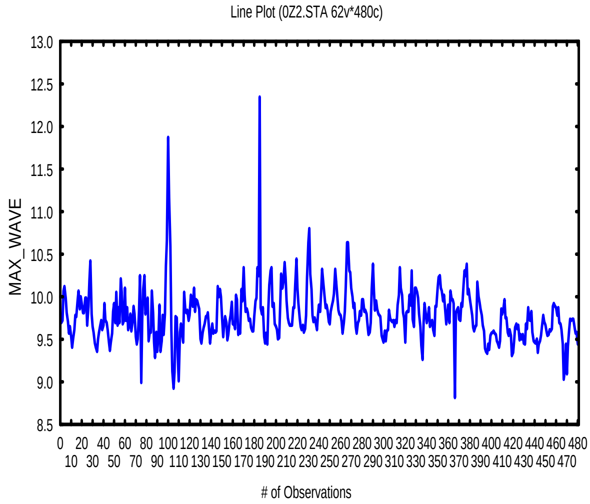

Figure 8. Monthly variation in maximum wavelength of emission due to Ozone layer depletion.

Y-axis = Maximum wavelength in μm
X-axis = time in month

It has been observed that human activities are increasing the contents of greenhouse gases in the atmosphere. Among these gases, water vapor is the strongest contributor in reducing the transparency of the infrared window (8 μ to 12 μ). Actually human beings do not directly influence the concentration of water vapor in the atmosphere. Due to the increase in the average global temperature, the average moisture content of the atmosphere is increasing. Consequently, this increases cloudiness. Figure 10 shows variation of wavelength vs the depletion of ozone [13-16].

Trend equation

$Y = 12.47 - 7.126\ X + \varepsilon$

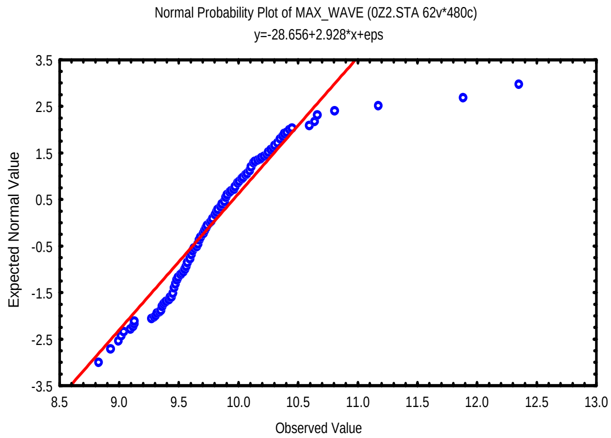

Figure 9. Normal distribution for maximum wavelength of emission due to Ozone layer depletion.

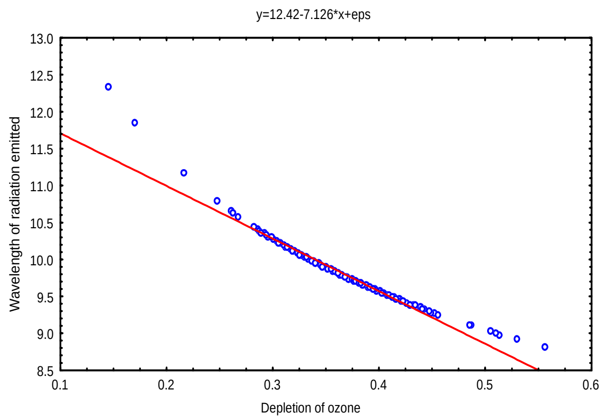

Figure 10. Variation in maximum wavelengths with increase in depletion of ozone concentration.

6. Predicting the Variability of Maximum Wavelength

We have established in our previous work in section 4 that AR(1) is an appropriate model for ozone layer depletion.

$X_t = \beta_1 X_{t-1} + \alpha_t$ or 0.934 ± 0.0035 and the Mean Sum of Squared Errors (MSSE) $\hat{\sigma}_a^2$ appears as 07.64 ± 0.9.

The most important window is the two-part window between 8 μ to 12 μ. This causes photons to interact with gas molecule and with cloud droplet or with fine-particles. A gas molecule absorbs photons if the gas molecule can make an internal rearrangement that requires the same amount of energy as that carried by the photon. This phenomenon is known as “tuning or resonance”. This accelerates the chemical dynamics of the region.

7. Conclusion

In this communication we have constructed a model for maximum wavelength of emission using the models of flux reaching Arabian Sea and mentioned in Eq. (8) and the Sea Surface Temperature as given in the Eq (11). Prediction equation of max wavelength has been evaluated using stochastic model of autoregressive nature for determining the variability in the structures of the emitted wavelength and results are having good accuracy limits.

Acknowledgement

We would like to thank the technical staff of Geophysical Center Quetta for providing data of ozone layer thickness for the specified period recorded by Dobson Spectrophotometer.

References

[1] C. Smith, Environmental Physics, Routledge, London (2004).

[2] O. P Neill, Environmental Chemistry, Chapman & Hall, New York (1993).

[3] M.P. Smith & K. Warr, Global Environmental Issues, Hodder and Stoughton, the Open University, London (1994).

[4] R. Guzzi, A. Navarra & T. Shukla, in Proceedings of the Course on Physical Climatology and Meteorology for Environmental Sciences, International Centre for Theoretical Physics (ICTP), World Scientific, Singapore, London and New Jersy (1988) pp.791-808

[5] G. Reinsel, C. G. Tiao, M. N. Wang, R. Lewis and D. Nychka, Atmos. Eng. **15** (1981) 1569.

[6] J. H. Seinfeld and N. S. Pandis, Atmospheric Chemistry and Physics, New York, John Wiley (1998).

[7] J. L. Thibodeaux, Environmental Chemodynamics, Movement of Chemicals in Air, Water and Soil New York, J. Wiley (1996).

[8] M.R. Schoch and L. M. Mckinney, “Environmental Science, Systems and Solutions”, Tennesee: Jones and Bartlett (1998).

[9] H. Tong, Nonlinear Time Series, A Dynamical System Approach, Oxford, Clarendon, (1990).

[10] R. S Stolarski and R J Cicerone, Can. J. Chem. **52** (1974) 1610.

[11] B. Kärcher, M. M. Hirschberg and P. Fabian, J. Geophys. Res.**101**, No.10 (1996) 15169.

[12] U. Feister and R. Grewe, Global and Planetary Change, **11**, No. 1 (1995) 25 Clarendon, Oxford.

[13] R. Garcia, Physics World **17** (1994) 49.

[14] M.A.K. Yousuf Zai and J Quamar, Indian J. Phys. **75**B, No.4 (2001) 307.

[15] M.A.K. Yousuf Zai, Ph.D Thesis submitted at the Institute of Space and Planetary Astrophysics University of Karachi (2003).

[16] C. Impey and W. K. Hartmann, The Universe Revealed, Pacific Grove, Brooks / Col, Chapter 12, New York (2000) p. 336.